PAPER

Channel Estimation Using Cyclic Delay Pilot for SC-MIMO Multiplexing

Takafumi FUJIMORI[†a)], **Kazuki TAKEDA**[†], ***Student Members***, **Kazuyuki OZAKI**[†], **Akinori NAKAJIMA**[†], ***Members***, ***and*** **Fumiyuki ADACHI**[†], ***Fellow***

SUMMARY In the next generation mobile communication systems, multiple-input multiple-output (MIMO) multiplexing is an indispensable technique to achieve very high-speed data transmission with a limited bandwidth. In MIMO multiplexing, it is necessary to estimate the channels between transmit and receive antennas for signal detection. In this paper, we propose a minimum mean square error (MMSE) channel estimation using cyclic delay pilot for single-carrier (SC)-MIMO multiplexing. In the proposed channel estimation, the same pilot block is altered through the addition of different cyclic delays and transmitted from different antennas at the same time for simultaneous estimation of all channels between transmit and receive antennas. We evaluate by computer simulation the bit error rate (BER) performance of MIMO multiplexing using the proposed channel estimation and compare it to those using time-multiplexed pilot based channel estimation (TMP-CE) and code-multiplexed pilot based channel estimation (CMP-CE).

key words: *MIMO multiplexing, channel estimation, cyclic delay*

1. Introduction

Broadband packet data services with a peak data rate of 100 M–1 Gbps are demanded in the next generation mobile communication systems [1], [2]. For such a high-speed packet transmission, the channels become severely frequency-selective and the bit error rate (BER) performance of single-carrier (SC) transmission degrades due to strong inter-symbol interference (ISI) [3]. Frequency-domain equalization (FDE) can significantly improve the SC transmission performance [4], [5]. To achieve very high-speed data transmission with a limited bandwidth, multiple-input multiple-output (MIMO) multiplexing technique has recently been attracting considerable attention [6], [7]. For SC-MIMO multiplexing, joint use of FDE and signal detection of parallel transmitted signals is essential [3]. In SC-MIMO multiplexing, an accurate estimation of channels between transmit and receive antennas is required.

A lot of pilot assisted channel estimation methods have been proposed for MIMO multiplexing [8], [9]. If different pilot blocks are transmitted simultaneously from transmit antennas, the channel estimation accuracy degrades due to inter-antenna interference (IAI). A channel estimation method proposed in [8] transmits the same pilot block sequentially from transmit antennas to estimate the channels between transmit and receive antennas without causing IAI. This is called time-multiplexed pilot based channel estimation (TMP-CE) in this paper. However, the pilot blocks must be transmitted the same number of times as the number of transmit antennas. In the case of a frequency-nonselective fading channel, orthogonal pilot blocks (i.e., Walsh codes) can be transmitted simultaneously from different antennas and the channels between transmit and receive antennas can be estimated at the same time [9]. This is called code-multiplexed pilot based channel estimation (CMP-CE) in this paper. However, in a frequency-selective fading channel, the channel estimation accuracy degrades due to the distortion of orthogonality among the pilot blocks.

Recently, channel estimation schemes without causing the orthogonality distortion in a frequency-selective fading channel were proposed for MIMO-orthogonal frequency division multiplexing (MIMO-OFDM) [9]–[11]. In [9], optimal pilot designs for MIMO-OFDM are presented. However, the channel estimation accuracy degrades if a certain number of the subcarriers are not used. The degradation due to the presence of null subcarriers can be mitigated by using the technique proposed in [10]. In [11], a channel estimation method using the carrier interferometry was proposed for MIMO-OFDM, which gives the linearly incremental phase rotation in frequency-domain to the pilot and uses zero-forcing (ZF) channel estimation. This pilot transmission is equivalent to those considered in [9], [10]. All the above channel estimation schemes [9]–[11] use ZF technique. However, ZF technique causes a problem in the case of SC-MIMO. This is because the frequency spectrum of the SC pilot (e.g., pseudo noise (PN) sequence) is, in general, not constant in frequency-domain, and therefore the ZF channel estimation produces noise enhancement. This problem can be solved by using Chu sequence whose spectrum is constant in frequency-domain, but the number of Chu sequences is limited. On the other hand, a fairly large number of pilot sequences are available if PN sequences are used. This leads to a very flexible choice of pilot sequences for channel estimation. Therefore, in this paper, we use PN sequences and propose a channel estimation scheme which can provide sufficiently accurate channel estimation independently of the pilot sequence used.

In this paper, we propose a minimum mean square error (MMSE) channel estimation scheme using cyclic delay pilot (called CDP-CE) for SC-MIMO. In CDP-CE, the same pilot block is altered through the addition of different cyclic

Manuscript received November 30, 2007.
Manuscript revised April 14, 2008.

[†]The authors are with the Department of Electrical and Communication Engineering, Graduate School of Engineering, Tohoku University, Sendai-shi, 980-8579 Japan.
a) E-mail: fujimori@mobile.ecei.tohoku.ac.jp

DOI: 10.1093/ietcom/e91–b.9.2925

delays and simultaneously transmitted from different antennas, similar to cyclic delay transmit diversity [12], [13], so that the channels between transmit and receive antennas can be simultaneously estimated without overlapping in delay time-domain.

The remainder of this paper is organized as follows. Section 2 describes SC-MIMO multiplexing. The CDP-CE is described in Sect. 3. Section 4 presents computer simulation results for the BER performance of SC-MIMO multiplexing with CDP-CE. Section 5 concludes the paper.

2. Overview of SC-MIMO Multiplexing

Figure 1 shows the transmitter/receiver structure of (N_t, N_r) SC-MIMO multiplexing, where N_t is the number of transmit antennas and N_r is that of receive antennas. In a frequency-nonselective fading channel, MMSE detection was proposed for the signal detection [3]. In this paper, we use the frequency-domain MMSE detection (MMSED) to mitigate the channel frequency-selectivity and to detect the signal. Figure 2 illustrates the frame structure for the proposed CDP-CE, CMP-CE, and TMP-CE. A group of N_p pilot blocks and N_d data blocks constitutes one frame. For CDP-CE and CMP-CE, a sequence of N_p pilot blocks is transmitted simultaneously from all N_t transmit antennas. However, for TMP-CE, the same pilot block is transmitted sequentially from N_t transmit antennas.

At the transmitter, a binary information sequence is converted into N_t parallel sequences by serial-to-parallel (S/P) conversion. Each binary information sequence is transformed into a data-modulated symbol sequence, which is then divided into a sequence of N_c-symbol blocks. The last N_g symbols in each block are copied and inserted as a cyclic prefix into the guard interval (GI). N_t parallel symbol blocks are transmitted simultaneously from N_t transmit antennas using the same carrier frequency.

At the receiver, a superposition of data blocks transmitted from N_t transmitted antennas is received by N_r antennas. The received signal $r_{n_r}(t)$, $t = -N_g \sim N_c - 1$, on the n_rth receive antenna can be expressed as

$$r_{n_r}(t) = \sqrt{2S} \sum_{n_t=0}^{N_t-1} \sum_{l=0}^{L-1} h_{n_r,n_t,l} d_{n_t}(t - \tau_l) + \eta_{n_r}(t), \tag{1}$$

where S is the average received signal power, $h_{n_r,n_t,l}$ and τ_l are respectively the path gain and the time delay of the lth path ($l = 0 \sim L-1$) between the n_tth transmit antenna and n_rth receive antenna, $d_{n_t}(t)$ is the transmitted signal from the n_tth transmit antenna, and $\eta_{n_r}(t)$ is a zero-mean noise process with variance $2\sigma^2 (= 2N_0/T)$. $1/T$ is the symbol rate per transmit antenna and N_0 is the one-sided power spectrum density of the additive white Gaussian noise (AWGN).

After removing the GI, the received signal block $\{r_{n_r}(t); t = 0 \sim N_c - 1\}$ is decomposed into N_c orthogonal frequency components $\{R_{n_r}(k); k = 0 \sim N_c - 1\}$ by applying N_c-point fast Fourier transform (FFT). $R_{n_r}(k)$ can be expressed as

$$R_{n_r}(k) = \sum_{n_t=0}^{N_t-1} H_{n_r,n_t}(k) D_{n_t}(k) + \Pi_{n_r}(k), \tag{2}$$

where $H_{n_r,n_t}(k)$ is the channel gain between the n_tth transmit antenna and the n_rth receive antenna, $D_{n_t}(k)$ is the signal component transmitted from the n_tth transmit antenna, and $\Pi_{n_r}(k)$ is a zero-mean complex Gaussian variable with variance $2N_c\sigma^2$. $D_{n_t}(k)$, $H_{n_r,n_t}(k)$ and $\Pi_{n_r}(k)$ are expressed as

$$\begin{cases} D_{n_t}(k) = \displaystyle\sum_{t=0}^{N_c-1} d_{n_t}(t) \exp\left(-j\frac{2\pi kt}{N_c}\right) \\ H_{n_r,n_t}(k) = \sqrt{2S} \displaystyle\sum_{l=0}^{L-1} h_{n_r,n_t,l} \exp\left(-j\frac{2\pi k\tau_l}{N_c}\right) \\ \Pi_{n_r}(k) = \displaystyle\sum_{t=0}^{N_c-1} \eta_{n_r}(t) \exp\left(-j\frac{2\pi kt}{N_c}\right) \end{cases}. \tag{3}$$

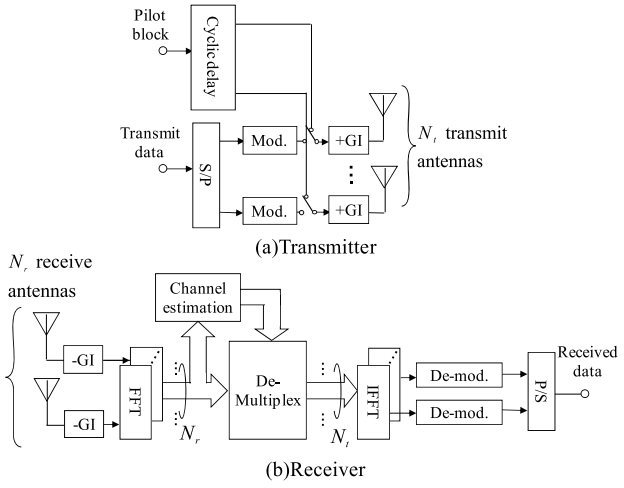

Fig. 1 (N_t, N_r) MIMO multiplexing.

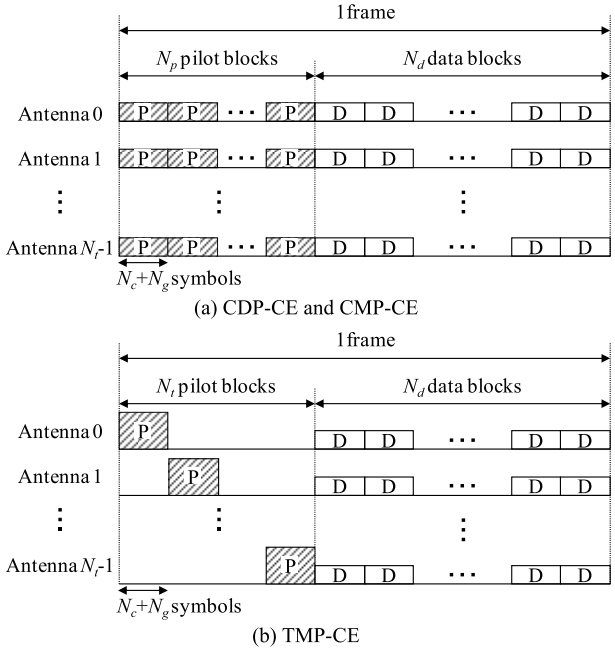

Fig. 2 Frame structure.

Equation (2) can be rewritten using the matrix representation as

$$\boldsymbol{R}(k) = \boldsymbol{H}(k)\boldsymbol{D}(k) + \boldsymbol{\Pi}(k), \tag{4}$$

where $\boldsymbol{R}(k)$ is the N_r-by-1 received signal vector, $\boldsymbol{H}(k) = \{H_{n_r,n_t}(k)\}$ is the N_r-by-N_t channel gain matrix, $\boldsymbol{D}(k) = \{D_{n_t}(k)\}$ is the N_t-by-1 transmitted signal vector, and $\boldsymbol{\Pi}(k) = \{\Pi_{n_r}(k)\}$ is the N_r-by-1 noise vector (whose elements are independent and identically distributed complex Gaussian variables).

The MMSED is applied to obtain the n_tth signal $\tilde{D}_{n_t}(k)$ as [3], [14]

$$\tilde{D}_{n_t}(k) = \boldsymbol{W}_{n_t}(k)\boldsymbol{R}(k), \tag{5}$$

where

$$\boldsymbol{W}_{n_t}(k) = \boldsymbol{H}^H_{n_t}(k)\left\{\boldsymbol{H}(k)\boldsymbol{H}^H(k) + 2\sigma^2\boldsymbol{I}_{N_r}\right\}^{-1} \tag{6}$$

with $\boldsymbol{H}_{n_t}(k)$ denoting the n_tth column vector of $\boldsymbol{H}(k)$, and $\boldsymbol{I}_{N_r}$ representing the N_r-by-N_r identity matrix. $(\cdot)^H$ is the Hermitian transpose operation. Next, N_c-point inverse FFT (IFFT) is applied to obtain the N_t parallel time-domain signal blocks, followed by data-demodulation to recover the transmitted binary information sequence.

Since $\boldsymbol{H}(k)$ and σ^2 are unknown to the receiver, they need to be estimated. The proposed CDP-CE will be described in Sect. 3.

3. MMSE Channel Estimation Using Cyclic Delay Pilot

3.1 Pilot Selection

The desired property of the pilot is that it has the constant amplitude in both time- and frequency-domains. Figure 3 illustrates the amplitude fluctuations of the spectrum of a PN sequence with a repetition period of 255 symbols and the Chu sequence [14]. The Chu sequence meets the requirement, but the number of Chu sequences is limited to 128 when $N_c = 256$. A fairly large number of pilot sequences are available if PN sequences are used. In this paper, we use PN sequences. Although a PN sequence has the constant amplitude property in time-domain, its amplitude varies in frequency-domain. This degrades the channel estimation accuracy if frequency-domain ZF channel estimation is used. Therefore, we apply MMSE channel estimation [15].

3.2 MMSE Channel Estimation

In CDP-CE, cyclic delay pilot is used. This is different from channel estimation schemes proposed in [9]–[11], which use the phase rotated pilot in frequency-domain. Since the amplitude of pilot varies in frequency-domain, the ZF channel estimation schemes presented in [9]–[11] degrade the channel estimation accuracy due to the noise enhancement. In this paper, we apply MMSE channel estimation and propose two types of CDP-CE. Type 1 uses the same PN pilot sequence for each pilot block. The channel estimation accuracy improves due to the noise averaging effect obtained by averaging the channel estimates over N_p pilot blocks. Type 2 uses a different PN pilot sequence for each pilot block so that the spectrum variation of pilot is smoothed out.

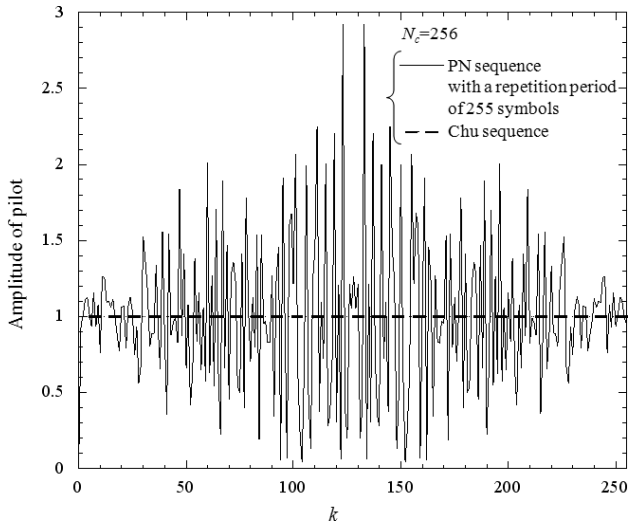

Fig. 3 Amplitude variations of pilot spectrum.

(a) Type 1

In the proposed channel estimation, a different cyclic delay (which is an integer multiple of GI length) is added to a different antenna. The ith pilot block $\{p^{(i)}(t);\ t = 0 \sim N_c - 1\}$, $i = 0 \sim N_p - 1$, to be transmitted from the n_tth transmit antenna is expressed as

$$p^{(i)}_{n_t}(t) = p^{(i)}((t - N_g n_t) \bmod N_c). \tag{7}$$

A superposition of N_t pilot blocks received on each receive antenna is decomposed by N_c-point FFT into the N_c orthogonal frequency components. The kth frequency component of $p^{(i)}_{n_t}(t)$ is given by

$$\begin{aligned} P^{(i)}_{n_t}(k) &= \sum_{t=0}^{N_c-1} p^{(i)}_{n_t}(t)\exp\left(-j\frac{2\pi kt}{N_c}\right) \\ &= P^{(i)}(k)\exp\left(-j\frac{2\pi kN_g n_t}{N_c}\right) \end{aligned} \tag{8}$$

and therefore, the kth frequency component of the ith received block can be expressed as

$$\begin{aligned} R^{(i)}_{n_r}(k) &= \left\{\sum_{n_t=0}^{N_t-1} H_{n_r,n_t}(k)\exp\left(-j\frac{2\pi kN_g n_t}{N_c}\right)\right\} \\ &\quad \times P^{(i)}(k) + \Pi^{(i)}_{n_r}(k), \end{aligned} \tag{9}$$

where $P^{(i)}(k)$ is the kth frequency component of the ith pilot block. The phase rotation in Eq. (8) is due to the addition of the cyclic delay to the pilot. Adding the cyclic delay is equivalent to giving the phase rotation in frequency-domain. We need to estimate $\boldsymbol{H}(k) = \{H_{n_r,n_t}(k);\ n_r = 0 \sim N_r - 1,\ n_t = 0 \sim N_t - 1\}$. This is done by MMSE-CE.

Figure 4 shows the proposed CDP-CE structure. First, MMSE-CE is performed to estimate the instantaneous composite channel gain as

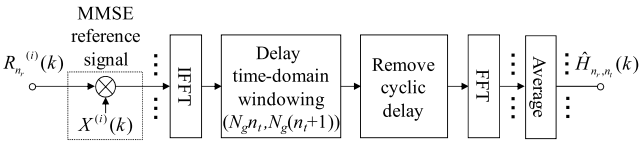

Fig. 4 CDP-CE structure.

$$\hat{H}_{n_r}^{(i)}(k) = X^{(i)}(k) R_{n_r}^{(i)}(k), \tag{10}$$

where $X^{(i)}(k)$ is the MMSE reference and $\hat{H}_{n_r}^{(i)}(k)$ is the composite channel gain between N_t transmit antennas and the n_rth receive antenna. From Eq. (9), the real composite channel gain $H_{n_r}(k)$ is expressed as

$$H_{n_r}(k) = \sum_{n_t=0}^{N_t-1} H_{n_r,n_t}(k) \exp\left(-j\frac{2\pi\, kN_g n_t}{N_c}\right). \tag{11}$$

$X^{(i)}(k)$ is determined so that mean square error (MSE) between $\hat{H}_{n_r}^{(i)}(k)$ and $H_{n_r}(k)$ is minimized. Defining the MSE $J_{n_r}(k)$ as

$$J_{n_r}(k) = E\left[\left|H_{n_r}(k) - \hat{H}_{n_r}^{(i)}(k)\right|^2\right], \tag{12}$$

and solving $\partial J_{n_r}(k)/\partial X^{(i)}(k) = 0$, we obtain the MMSE reference as

$$X^{(i)}(k) = \frac{\left\{P^{(i)}(k)\right\}^*}{\left|P^{(i)}(k)\right|^2 + \dfrac{N_c}{N_t}\left(\dfrac{S}{\sigma^2}\right)^{-1}}. \tag{13}$$

Next, N_c-point IFFT is applied to $\{\hat{H}_{n_r}^{(i)}(k);\ k = 0 \sim N_c - 1\}$ to obtain the composite channel impulse response estimate $\{\hat{h}_{n_r}^{(i)}(\tau);\ \tau = 0 \sim N_c - 1\}$. Since each transmit antenna is given a different cyclic delay of an integer multiple of GI length, the channel impulse responses associated with N_t transmit antennas do not overlap at all and can be discriminated. The channel impulse response $h_{n_r,n_t,l}$ between the n_tth transmit antenna and n_rth receive antenna appears in a delay time interval of $[N_g n_t, N_g(n_t + 1)]$. The cyclic delay incurred on the transmit antenna needs to be removed. The impulse response estimate $\{\hat{h}_{n_r,n_t}^{(i)}(\tau);\ \tau = 0 \sim N_c - 1\}$ can be obtained as

$$\hat{h}_{n_r,n_t}^{(i)}(\tau) = \begin{cases} \hat{h}_{n_r}^{(i)}(\tau + N_g n_t) & \text{if } 0 \le \tau < N_g \\ 0 & \text{otherwise} \end{cases}. \tag{14}$$

Finally, N_c-point FFT is applied to $\{\hat{h}_{n_r,n_t}^{(i)}(\tau);\ \tau = 0 \sim N_c - 1\}$ to obtain the channel gain estimates $\{\hat{H}_{n_r,n_t}^{(i)}(k);\ k = 0 \sim N_c - 1\}$.

Since N_p pilot blocks are transmitted from each antenna, N_p estimated channel gain matrices $\hat{\boldsymbol{H}}^{(i)}(k) = \{\hat{H}_{n_r,n_t}^{(i)}(k)\}$, $i = 0 \sim N_p - 1$, are obtained. They are averaged to obtain the final estimate. The final estimate is expressed as

$$\hat{\boldsymbol{H}}(k) = \frac{1}{N_p}\sum_{i=0}^{N_p-1} \hat{\boldsymbol{H}}^{(i)}(k). \tag{15}$$

The signal power S and noise power σ^2 in Eq. (13) are unknown to the receiver and must be estimated: they can be estimated according to [15]. S and σ^2 in Eq. (13) are replaced by the estimates, $\hat{S}$ and $\hat{\sigma}^2$, respectively. To compute the MMSED weight $\boldsymbol{W}_{n_t}(k)$ of Eq. (6), $\boldsymbol{H}(k)$ and σ^2 are replaced by their estimates, $\hat{\boldsymbol{H}}(k)$ and $\hat{\sigma}^2$, respectively.

(b) Type 2

In CDP-CE type 2, a different pilot sequence is transmitted in each pilot block. This means that each pilot block has a different frequency spectrum. Type 2 exploits this to improve the channel estimation accuracy. The channel estimation procedure of type 2 is identical to that of type 1 except for the MMSE reference $X^{(i)}(k)$.

$X^{(i)}(k)$ is determined so that MSE between $\frac{1}{N_p}\sum_{i=0}^{N_p-1} \hat{H}_{n_r}^{(i)}(k)$ and $H_{n_r}(k)$ is minimized. Defining the MSE $J_{n_r}(k)$ as

$$J_{n_r}(k) = E\left[\left|H_{n_r}(k) - \frac{1}{N_P}\sum_{i=0}^{N_p-1} \hat{H}_{n_r}^{(i)}(k)\right|^2\right] \tag{16}$$

and solving $\partial J_{n_r}(k)/\partial X^{(i)}(k) = 0$, we obtain the MMSE reference as

$$X^{(i)}(k) = \frac{N_p\left\{P^{(i)}(k)\right\}^*}{\displaystyle\sum_{j=0}^{N_p-1}\left|P^{(j)}(k)\right|^2 + \frac{N_c}{N_t}\left(\frac{S}{\sigma^2}\right)^{-1}}. \tag{17}$$

4. Computer Simulation

The simulation condition is summarized in Table 1. In this paper, we consider (4,4) MIMO multiplexing. We assume quadrature phase shift keying (QPSK) data modulation, a block length of $N_c = 256$ symbols, a GI length of $N_g = 32$ symbols, and an $L = 16$-path frequency-selective block Rayleigh fading channel having uniform power delay profile. The BER performance of SC-MIMO multiplexing using CDP-CE is compared with those using TMP-CE and CMP-CE. In TMP-CE, the delay time-domain windowing technique [15] is applied to reduce the noise. In CDP-CE type 1, only one PN pilot is used; the same PN pilot is transmitted in N_p pilot blocks from N_t antennas with different cyclic delays. In CDP-CE type 2, N_p different PN pilots are used; different one of N_p PN pilots is transmitted in each pilot block from N_t antennas with different cyclic delays. In CMP-CE, N_t different orthogonal pilots are used; each orthogonal pilot is constructed using a different Walsh sequence multiplied by a common PN sequence and N_t different orthogonal pilots are transmitted from N_t antennas in each pilot block. On the other hand, in TMP-CE, only one PN pilot is used similar to CDP-CE type 1. The pilot power is the same as the data block. In both CDP-CE and CMP-CE, the pilots are simultaneously transmitted from all transmit antennas, and so the transmit power is equally allocated to N_t pilot blocks. In TMP-CE, the N_t times larger transmit

Table 1 Simulation condition.

Transmitter	Data Modulation	QPSK 16QAM, 64QAM
	No. of Tx antennas	$N_t = 4$
	No. of pilot blocks/frame	$N_p = 1 \sim 8$
	No. of data blocks/frame	$N_d = 12$
	FFT/IFFT block size	$N_c = 256$
	GI length	$N_g = 32$
Channel	Fading type	Frequency-selective block Rayleigh fading
	Power delay profile	L=16-path uniform
Receiver	No. of Rx antennas	$N_r = 4$

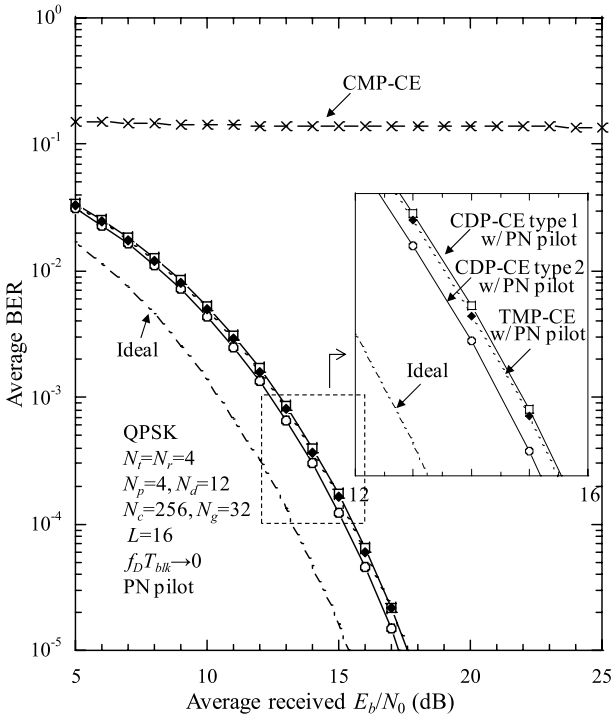

Fig. 5 Performance comparison between CDP-CE, TMP-CE and CMP-CE.

power is given to each pilot block because only one pilot block is transmitted from a different antenna at a different block time.

The BER performances are plotted for CDP-CE, TMP-CE and CMP-CE in Fig. 5 as a function of the average received signal energy per *information bit*-to-AWGN power spectrum density ratio E_b/N_0 ($= 0.5(ST/N_0)(1 + N_g/N_c)(1 + N_p/N_d)$) when the normalized maximum Doppler frequency $f_D T_{blk}$ ($= f_D(N_c + N_g)T$) $\rightarrow 0$, where T_{blk} denotes the block length in symbols. $N_t = N_r = 4$ is assumed. TMP-CE needs a transmission of $N_p = N_t$ pilot blocks. For fair comparison, we assume a transmission of $N_p = 4$ pilot blocks for

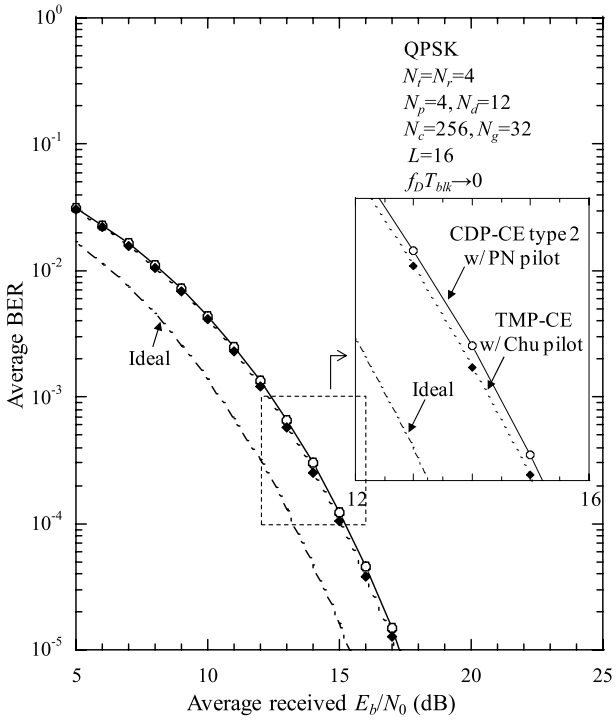

Fig. 6 Performance comparison between CDP-CE type 2 w/PN pilot and TMP-CE w/Chu pilot.

CDP-CE, TMP-CE, and CMP-CE (the pilot insertion loss is 1.25 dB). The BER performance for CMP-CE significantly degrades due to the distortion of orthogonality among the pilot blocks. On the other hand, since CDP-CE can retain orthogonality among the pilot blocks even in the frequency-selective fading channel, a good BER performance is obtained. CDP-CE type 1 provides almost the same BER performance as TMP-CE. However, CDP-CE type 1 slightly degrades from TMP-CE because the channel estimation accuracy degrades due to the IAI caused by using MMSE channel estimation. CDP-CE type 2 gives a better BER performance than both CDP-CE type 1 and TMP-CE since it smooths the variations of the pilot spectrum by averaging (see the denominator in Eq. (17)) and hence, improves the channel estimation accuracy. The E_b/N_0 loss for BER = 10^{-4} from the ideal channel estimation case is about 2.3 dB for CDP-CE type 1 and is about 2.2 dB and 1.9 dB for TMP-CE and CDP-CE type 2, respectively (including the pilot and GI insertion loss).

Chu pilot sequence has the constant spectrum and provides a good channel estimation accuracy. Figure 6 compares the BER performances achievable by CDP-CE type 2 with PN pilot and TMP-CE with Chu pilot. It can be seen from Fig. 6 that although the spectrum of PN pilot is not constant, CDP-CE type 2 with PN pilot provides almost the same BER performance as TMP-CE with Chu pilot.

In CDP-CE, cyclic delay-incurred pilot blocks are transmitted from all N_t transmit antennas simultaneously. The channel impulse responses associated with N_t transmit antennas can be separated in delay time-domain and hence,

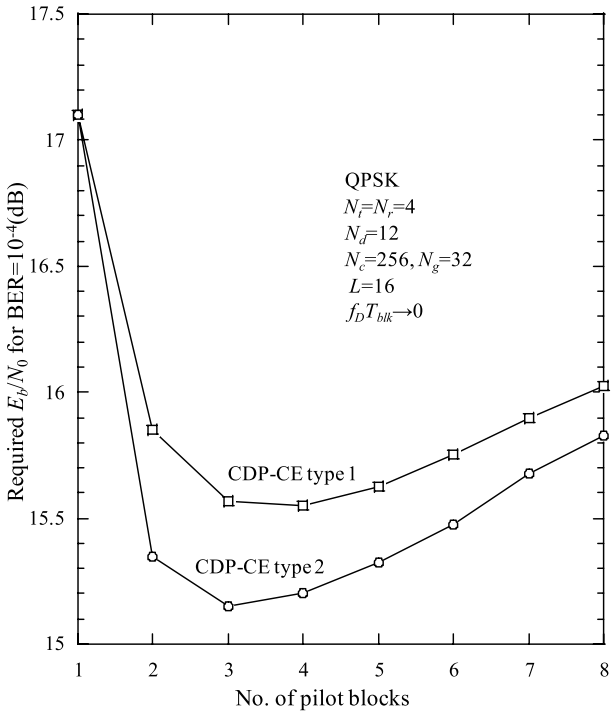

Fig. 7 Impact of N_p for CDP-CE.

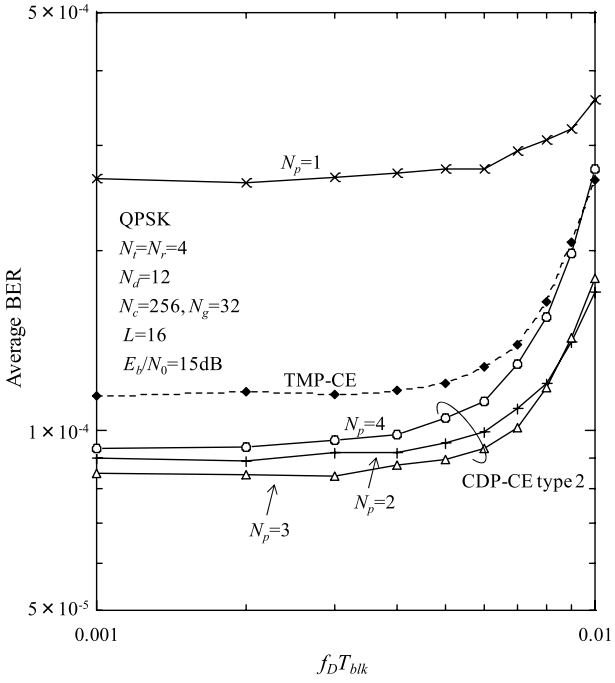

Fig. 8 Impact of fading maximum Doppler frequency.

the channels between transmit and receive antennas can simultaneously be estimated. Therefore, the number of pilot blocks is not necessary to be the same as that of transmit antennas and so, the pilot design is easier than TMP-CE. The channel estimation accuracy depends on the number of pilot blocks. Figure 7 plots the required E_b/N_0 for BER = 10^{-4} as a function of the number N_p of pilot blocks when $f_DT_{blk} \to 0$. As N_p increases, the required E_b/N_0 reduces due to the noise averaging effect for CDP-CE type 1 and due to the pilot spectrum and noise averaging effect for CDP-CE type 2, but starts to increase due to the increased pilot insertion loss if N_p increases beyond $N_p = 4$ for type 1 and $N_p = 3$ for type 2. Although the optimum N_p that minimizes the required E_b/N_0 is different between CDP-CE type 1 and 2, $N_p = 2$ can be used because it provides only a slight degradation of the required E_b/N_0. This means that CDP-CE can reduce the number of pilot blocks to less than that TMP-CE requires. CDP-CE type 1 and type 2 can provide the same or a better performance respectively by using the number of pilot blocks that is less than that for TMP-CE.

So far, we have considered the case where the channel gains stay constant over the period of N_p pilot blocks (i.e., very slow fading). Below, we will consider the case where the channel gains stay constant over each pilot block but vary block-by-block (i.e., fast fading). In Fig. 8, the impact of fading maximum Doppler frequency is shown for E_b/N_0 = 15 dB. $f_DT_{blk} = 0.001$ corresponds to the case of a symbol rate of 100 Msps, carrier frequency of 5 GHz, and a terminal moving speed of 75 km/h. Linear interpolation technique is applied to better track the channel variation. For the f_DT_{blk} value, as N_p increases, the BER first reduces due to the noise averaging effect, but starts to increase because the tracking ability against fading tends to be lost. It can be seen from Fig. 8 that $N_p = 3$ can be used for CDP-CE to achieve a good tracking ability against fading for a wide range of f_DT_{blk}.

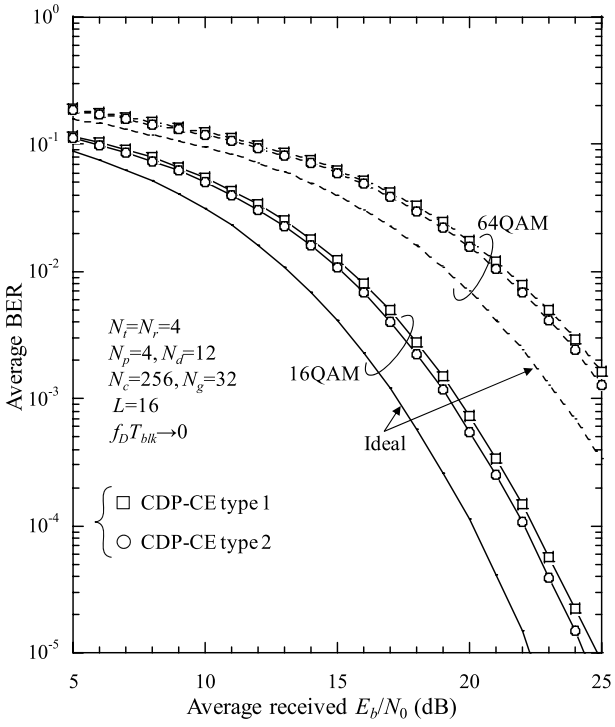

Fig. 9 BER performance when 16QAM and 64QAM are used.

In Fig. 9, the BER performances of CDP-CE type 1 and type 2 are plotted when higher level modulation is used (i.e.,

16QAM or 64QAM). CDP-CE type 2 provides a better performance than CDP-CE type 1. The E_b/N_0 loss for BER = 10^{-4} from the ideal channel estimation case is about 2.3 dB and 2.0 dB for type 1 and type 2, respectively.

5. Conclusion

In this paper, we proposed a channel estimation scheme using cyclic delay pilot (called CDP-CE) for SC-MIMO multiplexing and evaluated by computer simulation the achievable BER performance of (4,4) MIMO multiplexing. In CDP-CE, by using cyclic delay pilot, the channels between transmit and receive antennas can be simultaneously estimated. Two types of CDP-CE were proposed. Type 1 can reduce the noise by averaging the channel estimates. Type 2 can reduce the channel estimation error due to the pilot amplitude variation in frequency-domain as well as reduce the noise. It was shown by computer simulation that, using the transmission of $N_p = 4$ pilot blocks, CDP-CE type 2 provides a better BER performance than both CDP-CE type 1 and TMP-CE. Furthermore, it was shown that the number of pilot blocks can be reduced to $N_p = 3$ at the cost of only a slight performance degradation.

References

[1] H. Kawai, K. Higuchi, N. Maeda, M. Sawahashi, T. Ito, Y. Kakura, A. Ushirokawa, and H. Seki, "Likelihood function for QRM-MLD suitable for soft-decision turbo decoding and its performance for OFCDM MIMO multiplexing in multipath fading channel," IEICE Trans. Commun., vol.E88-B, no.1, pp.47–57, Jan. 2005.
[2] K. Higuchi, H. Kawai, N. Maeda, H. Taoka, and M. Sawahashi, "Experiments on real time 1-Gb/s packet transmission using MLD-based signal detection in MIMO-OFDM broadband radio access," IEEE J. Sel. Areas Commun., vol.24, no.6, pp.1141–1153, June 2006.
[3] J.G. Proakis, Digital communications, 4th ed., McGraw-Hill, 2001.
[4] D. Falconer, S.L. Ariyavisitakul, A. Benyamin-Seeyar, and B. Eidson, "Frequency domain equalization for single-carrier broadband wireless systems," IEEE Commun. Mag., vol.40, no.4, pp.58–66, April 2002.
[5] F. Adachi, D. Garg, S. Takaoka, and K. Takeda, "Broadband CDMA techniques," IEEE Wirel. Commun. Mag., vol.12, no.2, pp.8–18, April 2005.
[6] A. Van Zelst, R. Van Nee, and G. Awater, "Space division multiplexing for OFDM systems," Proc. 2000 IEEE Veh. Tech. Conf. (VTC), vol.2, pp.1070–1074, May 2000.
[7] T. Ohgane, T. Nishimura, and Y. Ogawa, "Applications of space division multiplexing and those performance in a MIMO channel," IEICE Trans. Commun., vol.E88-B, no.5, pp.1843–1851, May 2005.
[8] N. Egashira, H. Takayama, and T. Saba, "Improvement of CCI and residual frequency offset compensation using feedback phase tracking in MIMO-OFDM systems," IEICE Trans. Commun., vol.E90-B, no.4, pp.934–942, April 2007.
[9] I. Barhumi, G. Leus, and M. Moonen, "Optimal training design for MIMO OFDM systems in mobile wireless channels," IEEE Trans. Signal Process., vol.51, no.6, pp.1615–1624, June 2003.
[10] B. Le Saux, M. Helard, and R. Legouable, "Robust time domain channel estimation for MIMO-OFDMA downlink system," Proc. 6th International Workshop on Multi-Carrier Spread-Spectrum (MC-SS), Herrsching, Germany, May 2007.
[11] K. Yokomakura, S. Sampei, H. Harada, and N. Morinaga, "A carrier interferometry based channel estimation technique for one-cell reuse MIMO-OFDM/TDMA cellular systems," Proc. 2006 IEEE VTC, vol.4, pp.1733–1737, Melbourne, Australia, May 2006.
[12] G. Bauch, "Differential modulation and cyclic delay diversity in orthogonal frequency-division multiplex," IEEE Trans. Commun., vol.54, no.5, pp.798–801, May 2006.
[13] R. Kawauchi, K. Takeda, and F. Adachi, "Space-time cyclic delay transmit diversity for a multi-code DS-CDMA signal with frequency-domain equalization," IEICE Trans. Commun., vol.E90-B, no.3, pp.591–596, March 2007.
[14] D.C. Chu, "Polyphase codes with good periodic correlation properties," IEEE Trans. Inf. Theory, vol.5, no.7, pp.531–532, July 1972.
[15] K. Takeda and F. Adachi, "SNR estimation for pilot-assisted frequency-domain MMSE channel estimation," Proc. IEEE VTS APWCS, pp.4–5, Hokkaido University, Japan, Aug. 2005.

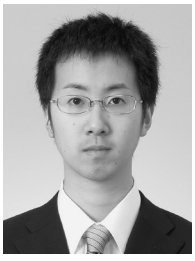

Takafumi Fujimori received his B.S. degree in communications engineering from Tohoku University, Sendai, Japan, in 2007. Currently he is a graduate student at the Department of Electrical and Communications Engineering, Tohoku University. His research interests include channel estimation for MIMO multiplexing.

Kazuki Takeda received his B.S. degree in communications engineering from Tohoku University, Sendai, Japan, in 2006. Currently he is a graduate student at the Department of Electrical and Communications Engineering, Tohoku University. His research interests include precoding and channel equalization techniques for mobile communication systems. He was a recipient of the 2007 IEICE RCS (Radio Communication Systems) Active Research Award.

Kazuyuki Ozaki received the B.S. and M.S. degrees in communication engineering from Tohoku University, Sendai, Japan, in 2005 and 2007, respectively. Since April 2007, he has been with Fujitsu Laboratories Limited, Yokosuka, Japan. His research interests include digital signal transmission techniques for multiple antenna system.

Akinori Nakajima received his B.S., M.S. and Dr.Eng. degrees in communications engineering from Tohoku University, Sendai, Japan, in 2002, 2004 and 2007, respectively. Since April 2007, he has been with Mitsubishi Electric Corporations, Kamakura, Japan. His research interests include MIMO, interference cancellation, equalization, Hybrid ARQ. He was a recipient of the 2005 IEICE RCS (Radio Communication Systems) Active Research Award.

Fumiyuki Adachi received the B.S. and Dr.Eng. degrees in electrical engineering from Tohoku University, Sendai, Japan, in 1973 and 1984, respectively. In April 1973, he joined the Electrical Communications Laboratories of Nippon Telegraph & Telephone Corporation (now NTT) and conducted various types of research related to digital cellular mobile communications. From July 1992 to December 1999, he was with NTT Mobile Communications Network, Inc. (now NTT DoCoMo, Inc.), where he led a research group on wideband/broadband CDMA wireless access for IMT-2000 and beyond. Since January 2000, he has been with Tohoku University, Sendai, Japan, where he is a Professor of Electrical and Communication Engineering at the Graduate School of Engineering. His research interests are in CDMA wireless access techniques, equalization, transmit/receive antenna diversity, MIMO, adaptive transmission, and channel coding, with particular application to broadband wireless communications systems. From October 1984 to September 1985, he was a United Kingdom SERC Visiting Research Fellow in the Department of Electrical Engineering and Electronics at Liverpool University. He was a co-recipient of the IEICE Transactions best paper of the year award 1996 and again 1998 and, also a recipient of Achievement award 2003. He is an IEEE Fellow and was a co-recipient of the IEEE Vehicular Technology Transactions best paper of the year award 1980 and again 1990 and also a recipient of Avant Garde award 2000. He was a recipient of Thomson Scientific Research Front Award 2004.